(35) B. Mayoh and P. Day, *Inorg. Chem.*, **13**, 2273 (1974); *J. Am. Chem. Soc.*, **94**, 2885 (1972).
(36) (a) J. B. Hasted, *Dielectr. Relat. Mol. Processes*, **1**, Chapter 5 (1972); (b) R. Pottel and U. Kaatze, *Ber. Bunsenges. Phys. Chem.*, **73**, 437 (1968).
(37) M. J. Powers, Ph.D. Dissertation, The University of North Carolina, Chapel Hill, N.C., 1977.
(38) Cannon has derived a different expression for λ_o by treating ligand-bridged mixed-valence ions as prolate ellipsoids having the major cylindrical axis along the line joining the metal centers (R. D. Cannon, *Chem. Phys. Lett.*, **49**, 299 (1977)).
(39) E_{op} at the intercept corresponds experimentally to a measurement in a nonpolar solvent like CCl_4 where $n^2 \approx D_s$.
(40) L. H. Vogt, J. L. Katz, and S. E. Wiberly, *Inorg. Chem.*, **4**, 1152 (1965).
(41) J. C. Solenberger, Ph.D. Dissertation, Washington University, St. Louis, Mo., 1970.
(42) M. J. Powers and T. J. Meyer, *J. Am. Chem. Soc.*, in press.
(43) Calculated as described above, except using $a_1 = [5(7.1)\ \text{Å} + 5.6\ \text{Å}]/6 = 6.9\ \text{Å}$
(44) D. J. Salmon, Ph.D. Dissertation, The University of North Carolina, Chapel Hill, N.C., 1976.
(45) J. K. Beattie, N. S. Hush, and P. R. Taylor, *Inorg. Chem.*, **15**, 992 (1976).
(46) C. Creutz and H. Taube, *J. Am. Chem. Soc.*, **95**, 1086 (1973).
(47) M. Davies, *Q. Rev., Chem. Soc.*, **8**, 250 (1954).
(48) W. C. Price, *Annu. Rev. Phys. Chem.*, **11**, 133 (1960).
(49) C. P. Smythe, "Dielectric Behavior and Structure", McGraw-Hill, New York, N.Y., 1955.

Contribution from the Department of Chemistry, Stanford University, Stanford, California 94305

μ-Pyrazine Polynuclear Mixed-Valence Species Based on Trans Ruthenium Tetraammines

A. VON KAMEKE, G. M. TOM, and H. TAUBE*

Received June 6, 1977

Polynuclear μ-pyrazine complexes based on *trans*-tetraammineruthenium as the linking metal unit have been prepared in two series. In one, ammonia occupies the terminal trans position and in this series the number of ruthenium atoms, n, ranges from 3 to 6. In the other series, with n = 2, 3, and 4, the terminal trans ligand is pyrazine. For the ammonia capped series, cyclic voltammetry indicates that the terminal ruthenium atoms are oxidized first. In this series, only when n = 3 does the near-IR absorption give evidence of end-to-end electron transfer in the one-electron oxidation product of the fully reduced species. For this system, the fact that the conproportionation constant of 70 much exceeds the statistical value also points to the conclusion that there is end-to-end communication. The mixed-valence species derived from both series show absorption in the near-infrared, usually complicated by the possibility of more than one metal-to-metal charge-transfer process. As the chain length increases, the absorption for the fully reduced state corresponding to the $\pi^* \leftarrow \pi$d transition moves progressively to lower energy, reaching 726 nm for the species with n = 6. On oxidation, this absorption moves to higher energies and at the same time it decreases in intensity, finally disappearing in the fully oxidized state.

Introduction

In the study of mixed-valence molecules, it is of interest to bridge the gap between our understanding of electron transfer in simple chemical reactions and electron transfer as it is encountered in extended arrays of atoms such as semiconductors and conductors. There is hope of achieving this by the study of polynuclear mixed-valence molecules. Results for several such systems have already been described: with pyrazine (pz) as bridging group and $Ru(bpy)_2$ as the metal core,[1,2] the mixed-valence species derived from $[[(NH_3)_5Ru(L)]_2Ru(bpy)_2]^{6+}$ by oxidation,[3] and polyferrocene species.[4] The systems we describe are most closely related to those reported on in the first three references and the Creutz ion itself.[5] In our systems, pyrazine is the bridging group and each ruthenium bears at most two π-acid ligands. Other work[6] has shown that the properties of the Creutz ion are dramatically altered when most of the saturated ligands are replaced by unsaturated ones.

Our investigations have included species with as many as six ruthenium atoms linked by pyrazine. Covering as they have a large number of species, they are incomplete in important respects, but we believe that the descriptions of the preparations and of general properties warrant publication at this stage.

Experimental Section

Preparations. It is to be noted at the outset that efforts to link large units proved futile, and the strategy we followed in the first series involved the stepwise reactions of the neutral species *trans*-$[SO_3(NH_3)_4Ru(OH_2)]$ to form trans pyrazine capped species $[Hpz(Ru(NH_3)_4pz)_nH]^{2n+2}$ where n ranges from 1 to 4. Sulfite labilizes the trans position, so that substitution takes place readily (it must be remembered, however, that this labilization is accompanied by a much reduced affinity).[7] On acidifying a solution containing a ruthenium sulfito complex and oxidizing with H_2O_2, SO_3^{2-} is converted to SO_4^{2-}. When the resulting species is reduced, SO_4^{2-} is replaced by water, and this ligand in turn is replaced by pyrazine. The source of the sulfito complex is $[SO_2Ru(NH_3)_4Cl]Cl$.[8] The species $[(NH_3)_5Ru(pz)(Ru(NH_3)_4pz)_mRu(NH_3)_5]^{2n+4}$ with m = 1–4 were then prepared by the reaction of $(NH_3)_5RuOH_2^{2+}$ with the appropriate pyrazine capped complex. The methods of preparation ensure that all the species we have studied are trans. Argon was used for deaeration in all the procedures which are described.

[*trans*-$Ru(NH_3)_4(pzH)_2]Cl_4$. Three hundred milligrams of *trans*-$[Ru(NH_3)_4(SO_2)Cl]Cl$ and an equal weight of pyrazine (pz) were dissolved in 4 mL of deaerated water, and the pH was adjusted to 7–8 using $NaHCO_3$. The solution was left for 5–10 min in the dark, acidified to about 1 M with HCl (no significant color change), and when CO_2 evolution had almost ceased, 30% H_2O_2 was added with stirring, until the color changed to a greenish brown. The mixture was added to a stirred solution of a 20-fold larger volume of concentrated HCl/acetone (1:19 by volume). Stirring was continued for several minutes and the solution was then cooled in the refrigerator for 1–2 h. The precipitate was collected, washed with acetone followed by ether, and dried in vacuo (yield >60%). The dried product has $[Ru(NH_3)(SO_4)pz]Cl$ as the major component. A total of 100 mg of the latter was dissolved in 2 mL of 0.01 M HCl and the solution was deaerated and reduced with zinc amalgam. Pyrazine (350 mg) was added, and after 2 h in the dark, the solution was poured into 2 mL of concentrated HCl + 40 mL of acetone while stirring. On storing in the refrigerator for 2 h, the precipitate was collected, washed with ether and acetone, and dried under vacuum (yield about 50%, without purification by gel filtration).

$[HpzRu_2pzH]Cl_6$. The first part of the preparation follows that just described except that 100 mg of $[Ru(NH_3)_4SO_2Cl]Cl$ and 12 mg of pyrazine were dissolved in 3 mL of deaerated water (after addition of $NaHCO_3$ the solution was dark red). The solid product of the oxidation by H_2O_2 (in this case the solution is yellowish green brown after a sufficient quantity of H_2O_2 is added) is $[SO_4Ru_2SO_4]Cl_2$

0020-1669/78/1317-1790$01.00/0

obtained in a 60 mg amount. The solid at this stage was light yellow-green. (If the operations after the addition of H_2O_2 are not done rapidly, some light brown impurities develop.) Of the latter, 100 mg was dissolved in 2 mL of 0.01 M HCl and after deaerating Zn(Hg) was added. On reduction, the solution has changed from a muddy yellow-green to violet (20 min), whereupon 350 mg of pyrazine was added and the mixture was allowed to stand for 2.5 h. This step and the succeeding ones were conducted with the reaction system shielded from light. The product solution, now blue-violet, was separated from the amalgam and was poured into 40 mL of concentrated HCl/acetone (1:20). After stirring for a few minutes, the solution was kept in the refrigerator for about 2 h. The solid was separated, washed with acetone and ether, and dried in vacuo. (The yield was about the same as above with slightly more impuities, mainly consisting of [*trans*-$Ru(NH_3)_4(pzH)_2]Cl_4$.)

Both $[Ru(NH_3)_4(pzH)_2]Cl_4$ and $[HpzRu_2pzH]Cl_6$ were purified by gel filtration. The column was packed with Bio-Gel P2 200–400 mesh supplied by Bio-Rad Laboratories; the solvent was 0.4 M HCl. Complexes were dissolved in a minimum of water, put on the column, and then eluted with 0.4 M HCl. The gel filtration was usually performed in air, but pressurization with nitrogen is desirable to accelerate the elution. The fraction containing the desired compound was collected and evaporated to dryness under vacuum. The solid which formed was dissolved in a minimum of water, precipitated using HCl/acetone (same proportions as above), and the precipitate was treated as described above.

$[HpzRu_3pzH]Cl_8$ or $[HpzRu_4pzH]Cl_{10}$. $[Ru(NH_3)_4(SO_2)Cl]Cl$ (300 mg) and 360 mg of $NaHCO_3$ were added to 5 mL of deaerated water, and after dissolution, 70 mg of $[Ru(NH_3)_4(pzH)_2]Cl_4$ or 60 mg of $[HpzRu_2pzH]Cl_6$ was added. The solution was kept in the dark for about 20 min, and then was diluted with deaerated water until all solid dissolved (trinuclear, about 20% volume increase; tetranuclear, up to 50%). After 5 min, the reaction solution, now an intense dark blue, was poured into 4–5 mL of ice-cooled concentrated HCl. The solution was stirred, and after CO_2 evolution was almost complete (10 s), 30% H_2O_2 was added dropwise until a greenish cast developed in the solution, whereupon a single volume containing a 10- to 20-fold excess of 30% H_2O_2 was added. The solution was then stirred without further cooling for about 3 min and filtered through a medium frit. The filtrate was promptly added to a 20-fold volume of concentrated HCl/acetone and stirred for about 5 min, and a few drops of 30% H_2O_2 was added. The product solution was kept in the refrigerator for 2 h, and the solid was separated, washed with acetone and ether, and dried in vacuo. At this stage, the solid has the composition $[O_4SRu_3SO_4]Cl_4$ or $[O_4SRu_4SO_4]Cl_6$.

For the next step 100 mg of solid was dissolved in a minimum of 0.1 M HCl (ca. 3 mL). The solution was deaerated and Zn(Hg) added. It was kept in the dark and after 0.5 h, a test for reduction was made. For this test, a drop of the reaction solution is diluted with deaerated water in a spectrophotometric cell. The cell is closed and the spectrum taken. If for the trinuclear a maximum appears at about 625 nm with a half-width of 100–120 nm, or if for the tetranuclear the maximum is just below 680 nm, with a half-width of 120–130 nm, the reduction is complete. When the test showed reduction to be complete, 300 mg of pyrazine/2 mL was added. One hour later, one-third the volume of 0.01 M HCl was added, which reduced the pH from ca. 5–6 to ca. 3 and a piece of Zn(Hg) was added, and the reaction continued, still in the dark for 2 h more. The product solution was transferred under argon to deaerated saturated NaCl, 1–2 M in HCl. The reaction flask was freed from occluded salt using the minimum volume of deaerated water, which was transferred to the NaCl solution. The final solution should be 60% saturated in NaCl for the trinuclear and 40–50% for the tetranuclear complex. The solution was mixed and deaerated by a stream of argon for 10 min and the vessel then closed and placed in the freezer overnight. The precipitate was collected under a blanket of argon using a fine frit. It was washed with cold deaerated water (0.5 mL) and 1 M HCl (1–3 mL) and then with acetone and ether and finally dried in vacuo.

$[NH_3Ru_3NH_3](OTs)_6$. In the first step $[SO_4Ru^{III}Ru^{III}NH_3]^{4+}$ was prepared, reduced, and converted to $[NH_3Ru_2pzH]^{5+}$. Sixty milligrams of *trans*-$[Ru(NH_3)_4(SO_2)Cl]Cl$ and 130 mg of $[Ru(NH_3)_5pzH](ClO_4)_3$ were mixed in 3 mL of deaerated water. Solid $NaHCO_3$ was added until the evolution of CO_2 ceased. After 10 min, 3 mL of concentrated HBF_4 was added and the mixture was cooled under argon in the freezer. The solid was separated and washed with 10 mL of ethanol/ether (1/4) and then dissolved in 10 mL of 1 M HCl and titrated with 30% H_2O_2 until the solution turned brown. The solution was filtered and a 20-fold volume of concentrated HCl/acetone (1/18) was added to the filtrate. After cooling, the solid was collected and washed with ethanol and ether. Yield was ca. 75%. The solid just prepared (137 mg) was dissolved in 7 mL of 1 M HCl and reduced in the dark with Zn(Hg) under argon. Pyrazine (400 mg) was added and the reaction was left to proceed for 4 h. The product solution was added to 3 mL of concentrated HCl in 60 mL of acetone, and the resulting mixture refrigerated for 72 h. The solid was collected, was washed with acetone and ether, and then was dissolved in 10 mL of 1 M HCl. Acetone (50 mL) was added to reprecipitate the yellow solid, which was collected and washed with acetone and ether.

The process yielded $[NH_3Ru_2pzH]Cl_5$. Of this 50 mg was added to a solution containing $[Ru(NH_3)_5Cl]Cl_2$ (100 mg) which had been reduced with Zn(Hg). After keeping the mixture in the dark for 5 h, it was transferred to a degassed flask containing 500 mg of HOTs and was kept in the freezer for ~2 h. The precipitate was collected by filtration (if done with dispatch, air need not be excluded), washed with a small amount of water and then ethanol/ether and ether, and dried in vacuo (yield, 60%).

$[NH_3Ru_nNH_3](Cl)_{2n}$ (n = 4, 5, 6). A solution containing 100 mg of $[Ru(NH_3)_5H_2O]Cl_2$ (prepared in situ by reduction of $[Ru(NH_3)_5Cl]Cl_2$) dissolved in 5 mL of deaerated water was added to about 25 mg of $[HpzRu_{n-2}pzH]Cl_{2n-2}$. Reaction continued in the dark for 2 h, whereupon pyrazine, severalfold in excess of $[Ru(NH_3)_5H_2O]^{2+}$, was added to convert it to $[Ru(NH_3)_5pz]^{2+}$ and the reaction continued for 1 h more. The solution was then transferred under argon to an equal volume of saturated NaCl–1 M HCl solution. From this point on, the procedure is the same as that described in the section devoted to $[HpzRu_3pzH]$.

For the preparation of the *p*-toluenesulfonate salts, the treatment with pyrazine to complex excess $[Ru(NH_3)_5H_2O]^{2+}$ is not necessary. After the 2 h reaction time, the solution is transferred into 100 mL of deaerated water. To this solution, a 1:1 mixture of HOTs and NaOTs is added until precipitation starts. The reaction mixture is refrigerated overnight; separation and further treatment of the solid follow procedures already described for the final stages of preparation.

A crucial step in the preparative procedure is the oxidation with H_2O_2, which is not easily reproducible. Changing the source of the H_2O_2 was found to affect the rates, and apparently impurities play a role. While for mononuclear species thus far studied, reaction with H_2O_2 leaves ruthenium in the (III) state, this is not necessarily the case for the polynuclear species of the present series in which Ru(II) is strongly stabilized by back-bonding. The reaction of H_2O_2 with substitution-inert ruthenium ammines is known to be very slow but is subject to catalysis.[10] The impurities may affect the state of oxidation of the complex after the treatment with H_2O_2 and thus its stability to decomposition by substitution.

It should be noted that the salts of the larger molecular weight species exhibit some unusual properties. When first precipitated they are often very voluminous, but shrink on drying to the expected small volumes.

The microanalytical data are summarized in Table I.

Some comments on the analyses are in order. Halide is low for most of the pyrazine capped species. Under the conditions of pre-

Table I. Summary of Microanalyses

Compound		Ru	C	N	H	X
$[Ru(NH_3)_4(pzH)_2]Cl_4$	Calcd	21.4	20.3	23.7	4.70	30.0
	Exptl	21.6	20.2	24.0	4.69	27.6[a]
$[HpzRu_2pzH]Cl_6$	Calcd	25.5	18.2	24.7	4.84	26.8
	Exptl	25.0	17.5	23.6	4.97	25.4[a]
$[HpzRu_3pzH]Cl_8$	Calcd	27.2	17.3	25.2	4.90	25.5
	Exptl	25.1	16.3	24.2	5.15	22.4[a]
$[HpzRu_4pzH]Cl_{10}$	Calcd	28.2	16.8	25.4	4.93	24.7
	Exptl	25.4	15.2	23.1	5.2	19.9[a]
$[(NH_3)Ru_3NH_3](OTs)_6$	Calcd	17.5	34.7	14.5	5.3	
	Exptl	17.0	33.8	14.0	5.2	
$[NH_3Ru_4NH_3](OTs)_8$	Calcd	17.4	35.2	14.5	5.31	11.1[b]
	Exptl	16.1	33.8	13.1	5.27	10.4
$[NH_3Ru_5NH_3](OTs)_{10}$	Calcd	17.4	35.5	14.4	5.27	
	Exptl	17.1	35.2	14.2	5.29	
$[NH_3Ru_6NH_3](OTs)_{12}$	Calcd	17.3	35.6	14.4	5.25	
	Exptl	16.5	34.5	13.1	5.14	

[a] X = Cl. [b] X = S.

Table II. Formal Reduction Potentials[a]

Species	E_f in V vs. NHE (peak-to-peak separation in mV)		
	$E(1)$	$E(2)$	$E(3)$
pzRu(pz)	0.85 (60)		
$pzRu_2pz$	0.81 (50)	0.90 (60)	
$pzRu_3pz$	0.83 (90)	0.96 (50)	
$pzRu_4pz$	0.83 (90)	0.96 (50)	
$NH_3Ru_3NH_3$	0.40 (70)	0.51 (70)	0.95 (60)
$NH_3Ru_4NH_3$	0.47 (100)	0.86 (70)	0.98 (70)
$NH_3Ru_5NH_3$[b]	0.48 (100)	0.62 (100)	0.97 (60)
$NH_3Ru_6NH_3$[b]	0.48 (-)	0.63 (90)	0.96 (100)

[a] In 1 M H_2SO_4 at ca. 20 °C. [b] Solubility low and maxima not pronounced.

cipitation protonation is incomplete and likely a mixture of fully and incompletely protonated compounds is precipitated. In many cases all the analyses, apart from H, are too low, but even in these the ratios conform, except for Cl and H, quite closely to theory. This point is illustrated with two of the preparations worst in this respect. (Ratio calcd for $[HpzRu_4pzH]Cl_{10}$: Ru, 4; C, 20; N, 26; H, 70; 10. Ratio found: Ru, 3.98; C, 20.0; N, 26.1, H, 82.1, Cl, 8.91. Calcd for $[NH_3Ru_5NH_3](OTs)_{10}$: Ru, 5; C, 86; N, 30; H, 152. Found: Ru, 4.91; C, 86.0; N, 29.7; H, 154.) In some cases, of which $[HpzRu_4pzH]Cl_{10}$ is an example, there was difficulty with moisture content, and, moreover, the solids containing the NH_3 capped species were slightly oxidized as was shown by examination of the spectra of solutions.

Finally, it should be noted that though successive members in the series when the number of ruthenium atoms is 3 or higher differ little in elemental analysis, in every case analytical results for the compounds cropped differ quite markedly from those of the precursor materials, which are the most likely impurities. The regular and reasonable gradation in properties, particularly with respect to the $\pi^* \leftarrow \pi d$ absorption, suggest that fairly good samples of the purported substances were in hand.

Results

Cyclic Voltammetry. The measurements were made in 1 M H_2SO_4 at ca. 20 °C, using carbon paste as the indicator electrode and saturated calomel as the standard with scan rates at 100–200 mV s^{-1}. All values of E_f have been corrected to NHE by adding 0.24 V to the mean of the oxidation and reduction waves which were registered. Owing to the symmetry of the species, for those containing three or more ruthenium atoms, it can be expected that some of the successive redox steps will nearly coincide in the values of E_f. An abnormal peak-to-peak separation is observed when the successive steps are close together and is a guide in identifying the processes in question. The results of the cyclic voltammetry measurements are summarized in Table II.

Absorption Spectra. Except for $[NH_3Ru_3NH_3](OTs)_6$, which was the most carefully investigated, and where standardized solutions were used in titrations, spectra were obtained by preparing a solution of the compound at a convenient concentration and then adding solid $(NH_4)_2Ce(NO_3)_6$ in weighed increments until the characteristic features of species containing the 2+ ruthenium had disappeared. This procedure is too crude to yield spectra of the intermediate stages of oxidation in a polynuclear complex. However, in every case, important features of the spectra of the early and final stages can be established, and some conclusions about the intermediate stages can also be reached.

A summary of the main absorption characteristics in the visible region of the fully reduced species is given in Table III. The spectra were obtained in water and at the prevailing concentrations the pyrazine capped species are unprotonated. The spectra in the visible region for $[pzRu(pz)]^{2+}$ and $[NH_3Ru_6NH_3]^{12+}$ are shown in Figure 1.

The oxidations were performed in 0.2 M HCl except for $[NH_3Ru_3NH_3](OTs)_6$ where 1 M H_2SO_4 was used. In 0.2 M HCl the pz capped ions are incompletely protonated and extent of protonation decreases with average oxidation state.

Table III. Absorption in the Visible Region

Species	λ_{max}, nm ($\epsilon \times 10^{-3}$, M^{-1} cm^{-1})[a]			Residual max[b]
pzRu(pz)	485[c] (11)	385 (1.0)	255 (7.0)	
$pzRu_2pz$	585[c] (43)	395 (3.0)	256 (17)	560
$pzRu_3pz$	659[c] (75)	460 (7.0)	257 (19.5)	585
$pzRu_4pz$	695 (104)	490 (10)	258 (25)	585
$NH_3Ru_3NH_3$	630 (25)			575
$NH_3Ru_4NH_3$	683 (91)	483 (9.0)	258 (22)	
$NH_3Ru_5NH_3$	710 (131)	515 (sh) (13)	262 (30)	580
$NH_3Ru_6NH_3$	726[d] (160)	535 (sh)[d] (15)	259 (40)	580

[a] For fully reduced species in water. [b] Maximum observed in 0.2 M HCl for the penultimate oxidized state. [c] In 0.2 M HCl, these peaks shift to 550, 605, and 660, for $pzRu_2pz$, $pzRu_3pz$, and $pzRu_3pz$, respectively. The change in medium produces virtually no shift in $pzRu_4pz$. [d] Maximum registered for purest sample prepared. Full spectrum registered only for a less pure sample which is the subject of Figure 1.

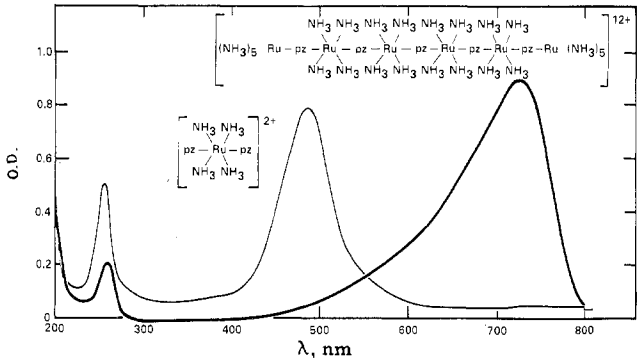

Figure 1. Spectra for $[pzRu(pz)]^{2+}$ and $[NH_3Ru_6NH_3]^{12}$ in the UV–visible region.

The strong visible band invariably moves to shorter wavelengths on oxidation before finally disappearing, and the weaker band as recorded in Table III also disappears or moves to shorter wavelength. Solid $(NH_4)_2Ce(NO_3)_6$ was chosen as the oxidant so as to avoid dilution of the solution, and it was not recognized at the time that NO_3^- under the conditions of the experiments involving long contact times can also act as oxidant. Even if no allowance is made for oxidation by NO_3^-, Ce(IV) in large excess is consumed, and it appears that in the last stages of the oxidation the complexes are being destroyed (it was shown that oxygen is not evolved). Despite this complication, the absorption maximum for the penultimate species short of complete oxidation could usually be identified. With the single exception of $NH_3Ru_4NH_3$, toward the last stages, over several increments of oxidant added, the absorption maximum remained at a fixed wavelength while it decreased in intensity. This wavelength was selected as the characteristic of the penultimate species. In the final stages, when the optical density had fallen to about 5% of the maximum, in most cases a further shift to the shorter wavelengths was observed, suggesting that low molecular weight species had been formed by degradation. It is possible that the deleterious side reactions may all be initiated by the reaction of nitrate ion. The features described are illustrated in Figure 2.

For none of the species is there significant absorption in the near-infrared in either the fully reduced or fully oxidized states,

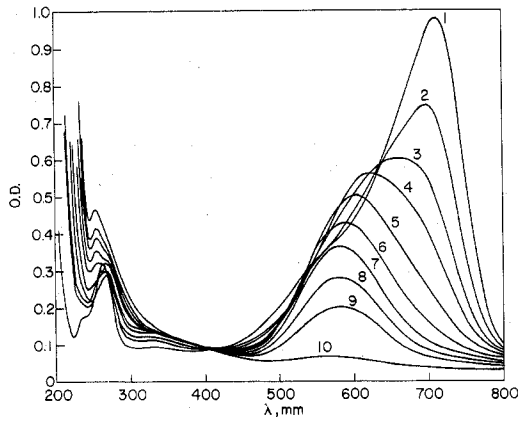

Figure 2. Change in spectrum of $[NH_3Ru_5NH_3]^{10+}$ on oxidation. Numbers refer to the addition of successive increments of oxidant, beginning with none for curve 1.

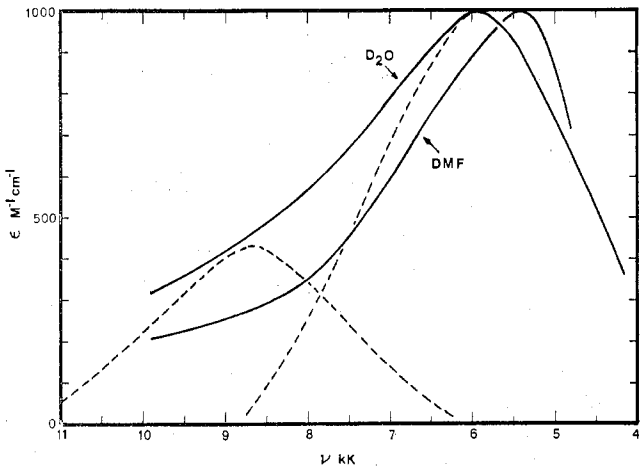

Figure 3. Spectrum of $NH_3Ru_3NH_3^{7+}$ in the near-infrared region in D_2O and DMF as solvents. Dotted lines show an attempted resolution into two bands for the spectrum in D_2O. (1 kK = 0.1 μm^{-1}.)

but all show strong absorption in this wavelength region in the intermediate oxidation states. Only for $NH_3Ru_3NH_3$ were the measurements done accurately enough to yield quantitative data for the intermediate oxidation states.

The absorption for a solution containing $[NH_3Ru_3NH_3]^{6+}$ to which exactly 1 equiv of oxidant/mol of complex has been added is shown in Figure 3. The band shape in D_2O, and more particularly the fact that the shape is sensitive to the change in solvent, indicates that the band is composite in character. This conclusion is strengthened by comparing the shapes for $[NH_3Ru_3NH_3]^{8+}$, Figure 4, with that for $[NH_3Ru_3NH_3]^{7+}$, the former being much more symmetrical. A resolution into two bands, admittedly only approximate, was arrived at by reflecting the low-energy branch for the 7+ ion in D_2O about an axis through the envelope maximum. A second band then emerges, but the maximum for it is difficult to fix because of a contribution from the $\pi d-\pi^*$ band in the high-energy region. The approximate assignments of the band maxima on this basis are $\nu_2 = 0.59$ μm^{-1} ($\Delta\nu_{1/2} = 0.28$ μm^{-1}) and $\nu_1 = 0.87$ μm^{-1} ($\Delta\nu_{1/2} = 0.28$ μm^{-1}). The change in shape on changing the solvent to DMF suggests that ν_1 is more sensitive to solvent than ν_2, and deconvolution for the latter solvent is even more difficult than it is for D_2O. The 8+ ion has band maxima at 0.99 (D_2O), 0.89 (DMF), and 0.88 μm^{-1} (Me_2SO), the extinction coefficient at the maximum being about 1.0×10^{-3} M^{-1} cm^{-1}.

For the remainder of the species, the spectra in the near-IR were run only in D_2O; Figure 5 shows the results of the titration of $[NH_3Ru_5NH_3]^{10+}$ with solid $(NH_4)_2Ce(NO_3)_6$. The

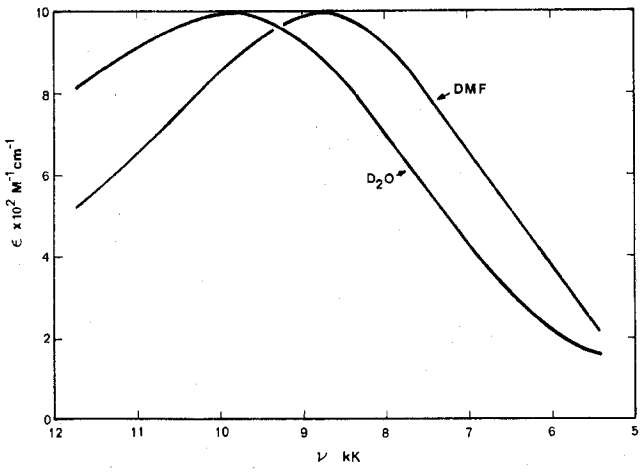

Figure 4. Near-infrared spectrum of $[NH_3Ru_3NH_3]^{8+}$ in D_2O and in DMF. (1 kK = 0.1 μm^{-1}.)

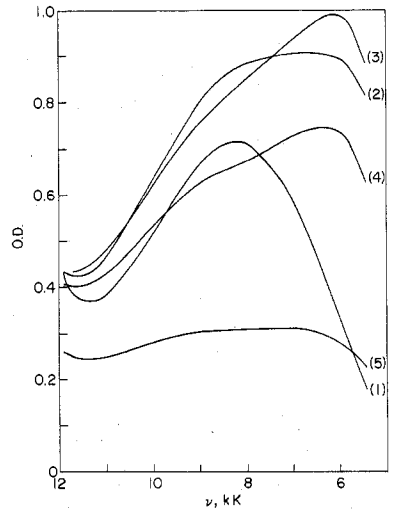

Figure 5. Near-infrared absorption for $NH_3Ru_5NH_3$ as a function of extent of oxidation (0.2 M HCl, ~20 °C). First increment added produces 1, successive increments as indicated by numbers. (1 kK = 0.1 μm^{-1}.)

behavior observed for $[NH_3Ru_4NH_3]^{8+}$ and $[NH_3Ru_6NH_3]^{12+}$ is in general similar. For these, in contrast to $[NH_3Ru_3NH_3]^{6+}$, the first increment of oxidant, in each case less than the amount required to produce the singly oxidized form, produces absorption only at higher energies, with no observable contribution from a low-energy band. On further oxidation, absorption does develop at lower energies, and the penultimate species show absorption over a wide range of wavelengths and are certainly composite in structure. It should be mentioned that for these species and the others to be described, the maximum absorption corresponds to extinction coefficients in excess of 1×10^3 M^{-1} cm^{-1}.

Turning now to the pz capped species, the spectrophotometric results in the near-infrared for $[pzRu_2pz]^{4+}$ and $[pzRu_4pz]^{6+}$ are shown in Figures 6 and 7. The observations in these cases are complicated by the fact that the species in intermediate oxidation states may exist in more than one state of protonation. Thus when $[pzRu_2pz]^{4+}$ is titrated, both $[pzRu_2pz]^{5+}$ and $[pzRu_2pzH]^{6+}$ are likely present, and the intervalence transition for the latter, which is unsymmetrical, is expected to be at higher energies than for the former. This may be the cause, at least in part, of the unsymmetrical band shape observed. The system is well behaved in other respects. An isosbestic point is observed (1.11 μm^{-1}) in the titration until the $[2,3]^{11}$ equivalence point is reached (note that the ratio of $[pzRu_2pz]^{5+}$ and $[pzRu_2pzH]^{6+}$ will remain unchanged

Table IV. Development of Near-IR Bands on Oxidation

Parent species	ν_{max} for 1st mixed-valence species, μm^{-1}	Response to further oxidation
$[pzRu_2pz]^{4+}$	0.61	
$[pzRu_3pz]^{6+}$	0.57	Abs. broadens to higher energies
$[pzRu_4pz]^{8+}$	<0.54	Max shifts slightly to higher energies
$[NH_3Ru_3NH_3]^{6+}$	0.59, 0.87	9.9 for 8+
$[NH_3Ru_4NH_3]^{8+}$	0.79	Band develops at lower energy. Final is broad, max at 9.5
$[NH_3Ru_5NH_3]^{10+}$	0.81	Band develops at lower energy. Final is very broad
$[NH_3Ru_6NH_3]^{12+}$	0.83	As above

during the titration), but beyond this point, the absorption decreases proportionately over the whole wavelength region. For the tri- and tetraruthenium species, the behavior is more complicated, as is expected when the number of distinguishable sites per molecule increases. There is a progressive shift in the early maximum toward lower energy as the number of ruthenium ions increases in this series and for the first oxidation product of $[pzRu_4pz]^{8+}$ the maximum lies below 0.54 μm^{-1}. For both the tri- and tetraruthenium species the maximum moves to higher energies as the oxidation progresses and eventually decreases in intensity.

Some of the observations bearing on the near-IR bands as described are summarized in Table IV.

Discussion

The ammonia capped species have the terminal atoms in an environment quite different from the remaining ones, and this simplifies the interpretation of at least some of the results. For $NH_3Ru_3NH_3$, the three values of E_f can confidently be assigned to the processes.

$$[3,3,3] \xrightarrow{0.95} [3,2,3] \xrightarrow{0.51} [3,2,2] \xrightarrow{0.40} [2,2,2]$$

Significant interaction between the terminal ruthenium atoms is indicated by the fact that the conproportionation constant (K_c = 70)

$$[3,2,3] + [2,2,2] = 2[3,2,2]$$

is considerably above the statistical value of 4. Even more compelling is the evidence from the near-IR absorption of the 7+ ion. Regardless of the validity of the deconvolution shown in Figure 3, the band maximum at 0.59 μm^{-1} can reasonably only be assigned to the symmetrical end-to-end intervalence transition [2,2,3] ← [3,2,2]. For the 8+ ion, only the unsymmetrical transition [2,3,3] ← [3,2,3] is possible, lying at higher energy because the central ruthenium is stabilized in the 2+ state relative to the terminal ones (note that it carries two pyrazines as ligands). The higher energy transition in the 7+ ion, if indeed there is one, is then assigned to [2,3,2] ← [3,2,2]. At any rate, it appears that the transition associated with end-to-end electron transfer has a high intensity, even though it takes place through what might be regarded as a saturated atom, namely Ru(II) in a low-spin d^6 configuration. However, the energy gap between the [2,2,3] and [2,3,2] states is not great and there will be a significant contribution of the latter to the ground state. In this connection, it is important to note that the mixed-valence [3,2,2] species derived from $[(NH_3)_5Ru(pz)Ru(bpy)_2pzRu(NH_3)_5]^{7+}$ does not show significant absorption at lower energies.[13] The difference from $[NH_3Ru_3NH_3]^{7+}$ is understandable on the basis that the πd levels in $Ru(bpy)_2$ are very much stabilized relative to those of the middle ruthenium in $NH_3Ru_3NH_3$ and thus there is little admixture of [2,3,2] to the ground state in the $Ru(bpy)_2$ case. It should also be noted that the two oxidation steps involving the end rutheniums on $(NH_3)_5Ru(pz)Ru(bpy)_2pzRu(NH_3)_5$ are *less* well resolved than they are in $NH_3Ru_3NH_3$, again indicating a weaker interaction between the end rutheniums in the former than in the latter case.

There seems to be some of the same difficulty in interpreting the low-energy transition in $[NH_3Ru_3NH_3]^{7+}$ as there is in assigning the near-IR band in the Creutz ion.[5,14,15] The bandwidth is less than calculated[12] (0.28 vs. 0.38 μm^{-1}), and considering the large distance between the outside metal ions, the change in band energy with solvent is not great. Another point to note is that if the near-IR transition in the Creutz ion and ν_2 in $[NH_3Ru_3NH_3]^{7+}$ were both normal intervalence transitions, the energy would be expected to be higher for the latter than the former, and this is not the case. If ν_2 were in fact a normal intervalence transition, an energy of the order of that observed[16] in $[(NH_3)_5Ru(4,4'\text{-bpy})Ru(NH_3)_5]^{5+}$ would be expected, namely, 0.96 μm^{-1} rather than 0.59 μm^{-1} as observed. It would appear then that $[NH_3Ru_3NH_3]^{7+}$ is valence delocalized in somewhat the sense that the Creutz ion is.

Elsewhere,[17] the large value of the conproportionation constant for the Creutz ion has been attributed mainly to an instability of the [2,2] state arising from the electronic repulsions attending back-bonding into a common orbital from two metal centers. These repulsions would be less severe in the $[NH_3Ru_3NH_3]^{6+}$, and thus a smaller conproportionation for the [3,2,2] would be expected than for the Creutz ion, in harmony with the observations.

For the remaining members of the NH_3 capped series, the cyclic voltammetry waves corresponding to the first two oxidation steps, which in each case undoubtedly involve the external ruthenium atoms, are not resolved, but that the waves are composite is manifested in the abnormally large peak-to-peak separations noted at least for the tetra- and pentaruthenium species (for the hexaruthenium, owing to low solubility, the peak-to-peak separations are difficult to measure). The peak-to-peak separations registered for $NH_3Ru_4NH_3$ are consistent with the reasonable expectation that the third and fourth oxidation steps each consist of a one-electron change. In $NH_3Ru_5NH_3$, the steps break up as 2, 2, and 1 and in $NH_3Ru_6NH_3$, as far as can be determined, as 2, 2, and 2. Only for the first among the three is there a significant difference between the potential required to oxidize pairs of ruthenium(II) ions which are equivalently located in the molecules. The values of E_f recorded in Table II for removing the third and fourth electrons from $NH_3Ru_4NH_3$ lead to a value of ca. 100 for the conproportionation constant of the reaction

$$[3,2,2,3] + [3,3,3,3] = 2[3,3,2,3]$$

A result of interest is that the absorption in the near-IR at low energy, which in the case of $[NH_3Ru_3NH_3]^{7+}$ we ascribe to an end-to-end communication, is so weak for the higher members of the NH_3 capped series as not to be observable. The near-IR maxima for $[NH_3Ru_4NH_3]^{9+}$, $[NH_3Ru_5NH_3]^{11+}$, and $[NH_3Ru_6NH_3]^{13+}$ appear at rather higher energies, 0.79, 0.815, and 0.83 μm^{-1}, respectively, as expected if they are associated with electron transfer between nonequivalent sites. On further oxidation of each of the three, near-IR absorption does develop at lower energies, and this presumably involves transitions within the core of the similarly coordinated inner ruthenium atoms.

In the pz capped species, the immediate environment around each metal ion is the same, and since pz provides for strong coupling between the ruthenium ions, it can be expected that the interpretation of the results encounter some of the same difficulties which are met in the Creutz ion. This clearly seems to be the case for $pzRu_2pz$. Figure 6 shows an anomalous band shape for the mixed-valence species derived from it which is reminiscent of that observed for the Creutz ion. The bandwidth at half-height measured in Figure 6 is 0.24 μm^{-1}; that

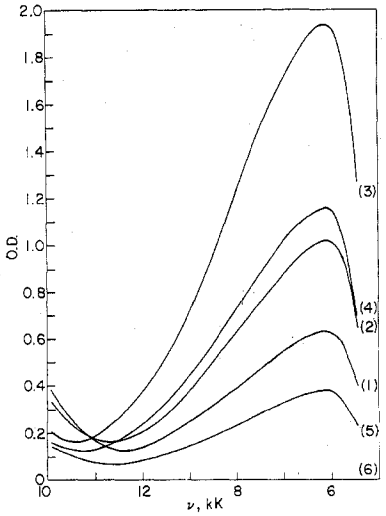

Figure 6. Near-infrared absorption for $pzRu_2pz$ as a function of extent of oxidation (0.2 M HCl, ~20 °C). First increment added produces 1, successive increments as indicated by numbers. (1 kK = 0.1 μm^{-1}.)

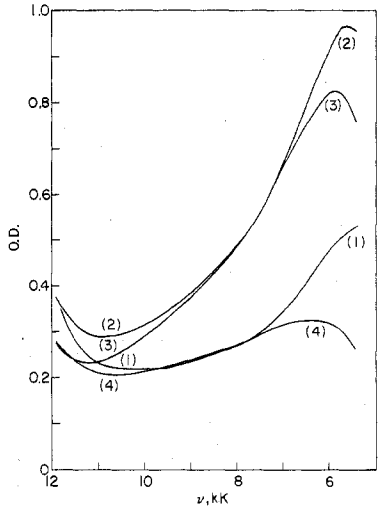

Figure 7. Near-infrared absorption for $pzRu_4pz$ as a function of extent of oxidation (0.2 M HCl, 20 °C). First increment added produces 1, successive increments as indicated by numbers. (1 kK = 0.1 μm^{-1}.)

calculated from the equation given by Hush[12] is 0.36 μm^{-1}. The discrepancy is really larger than is indicated by this comparison because the near-IR band for the mixed-valence ion is probably composite, and the "width" recorded is the gross width for the unsymmetrical band.

The fact that partial symmetric replacement of NH_3 by N heterocyclics in the Creutz ion moves the near-IR band to lower energies has already been pointed out,[5] and it is observed again in comparing the band maximum as shown in Figure 5 (0.615 μm^{-1}) with that reported for the Creutz ion in D_2O (0.635 μm^{-1}). This trend is particularly interesting in the face of the fact that extensive replacement of NH_3 by π-acid ligands moves the near-IR transition to *higher* energies.[6a] The change to higher energies is reasonable, if the coupling that causes the valence delocalization in the Creutz ion is the πd–π^* interaction. The auxiliary π-acid ligands compete with the bridging ligand for the πd electron density; this decreases the coupling and a valence-trapped species results. The shift to lower energies recorded for the mixed-valence ion derived from $[pzRu_2pz]^{4+}$ as compared to the Creutz ion is more difficult to understand.

Because the environments for the rutheniums in the pz capped species are so similar, different sites of oxidation are more difficult to distinguish than is the case for the ammonia capped systems. The greater peak-to-peak separation at E_f = 0.83 V than at E_f = 0.96 V for $HpzRu_3pzH$ suggests that the first oxidation act involves two equivalent sites, which then could well be the terminal ruthenium ions. A point of some concern is that the peak-to-peak separation for some of the cyclic voltammetry traces is less than the theoretical value of 59 mV for a one-electron change; cf. species $pzRu_2pz$ and $pzRu_3pz$. A small peak-to-peak separation is also observed for the second wave in $pzRu_4pz$, but now there is the possibility that the second wave involves what is nearly a two-electron change. This cannot, however, be the case for $pzRu_3pz$ if the first wave involves two successive one-electron steps. Where there is no possibility of a two-electron change, the small peak-to-peak separation implies adsorption on the electrode.

The near-IR bands for species $pzRu_3pz$ have the same general features in the early stages of oxidation as are shown in Figure 7 for $pzRu_4pz$ and are consistent with the view that the first oxidation makes possible a transition between equivalent sites and thus involves removal of an electron from a terminal ruthenium. On further oxidation, a higher energy component becomes prominent. In the final stage, the absorption is broad and symmetrical with a maximum at ca. 0.8 μm^{-1}. It probably corresponds to [3,2,3] for which only a single "intervalence transition" is possible—this statement is made with the qualification that the systems may be well in the direction of being valence delocalized. In the case of $pzRu_3pz$, a unique assignment of the oxidation stages is possible because of the particular symmetry but this is not the case for $pzRu_4pz$, where the molecule has two sets of equivalent sites.

Perhaps the most notable feature of the absorption for the species in the visible is the progressive shift of the band to lower energies as the length of the molecule increases. The shift to higher energies on oxidation, at least in the case of the NH_3 capped series, can be understood on the basis that, on oxidizing the terminal ruthenium ions, the chain of Ru–pz oscillators is shortened. The effect, as might be expected if the pz capped species were valence delocalized, is much less for them than for the ammonia capped series.

A number of questions arising from the data have been commented on. Others come readily to mind, but it appears that further experimental work will be necessary before it becomes profitable to dwell on them.

Acknowledgment. Support of this research by the NSF (Grant GP24726) and by the Deutsche Forschungsgemeinschaft (fellowship for A.v.K.) is gratefully acknowledged.

Registry No. $[Ru(NH_3)_4(pzH)_2]Cl_4$, 66358-73-4; $[HpzRu_2pzH]Cl_6$, 66358-55-2; $[HpzRu_3pzH]Cl_8$, 66358-56-3; $[HpzRu_4pzH]Cl_{10}$, 66358-57-4; $[NH_3Ru_3NH_3](OTs)_6$, 66358-59-6; $[NH_3Ru_4NH_3](OTs)_8$, 66358-61-0; $[NH_3Ru_5NH_3](OTs)_{10}$, 66358-63-2; $[NH_3Ru_6NH_3](OTs)_{12}$, 66358-65-4; $[NH_3Ru_3NH_3]^{7+}$, 66454-96-4; $[NH_3Ru_4NH_3]^{9+}$, 66454-97-5; $[NH_3Ru_5NH_3]^{11+}$, 66454-98-6; $[NH_3Ru_6NH_3]^{13+}$, 66454-99-7; $[NH_3Ru_3NH_3]^{8+}$, 66455-00-3; *trans*-$[Ru(NH_3)_4(SO_2)Cl]Cl$, 23346-07-8; H_2O_2, 7722-84-1; $[Ru(NH_3)_5H_2O]Cl_2$, 66402-61-7.

References and Notes

(1) S. A. Adeyemi, J. N. Braddock, G. M. Brown, J. A. Ferguson, F. J. Miller, and T. J. Meyer, *J. Am. Chem. Soc.*, **94**, 300 (1972).
(2) S. A. Adeyemi, B. C. Johnson, F. J. Miller, and T. J. Meyer, *Inorg. Chem.*, **12**, 2371 (1973).
(3) M. J. Powers, R. W. Callahan, D. J. Salmon, and T. J. Meyer, *Inorg. Chem.*, **15**, 894 (1976).
(4) G. M. Brown, T. J. Meyer, D. O. Cowan, C. LeVanda, F. Kaufman, P. V. Roling, and M. D. Rausch, *Inorg. Chem.*, **14**, 506 (1975).
(5) C. Creutz and H. Taube, *J. Am. Chem. Soc.*, **91**, 3988 (1969); **96**, 7827 (1974).
(6) (a) R. W. Callahan and T. J. Meyer, *Chem. Phys. Lett.*, **39**, 82 (1976); (b) R. W. Callahan, G. M. Brown, and T. J. Meyer, *Inorg. Chem.*, **14**, 1443 (1975).
(7) S. Isied and H. Taube, *Inorg. Chem.*, **13**, 1545 (1974).
(8) K. Gleu and K. Rehm, *Z. Anorg. Allg. Chem.*, **227**, 237 (1936).
(9) In the notation adopted, only the capping groups and the number of rutheniums are specified. It is understood that the rutheniums are separated by pyrazine and that ammonia molecules complete the co-

ordination sphere about Ru to 6. For the pz-capped species in acid solution particularly on oxidation, there is ambiguity about the state of protonation. OTs represents toluenesulfonate; pz, pyrazine.
(10) J. R. Pladziewicz and H. Taube, *Inorg. Chem.*, **12**, 639 (1973).
(11) This notation represents a formal assignment of oxidation state and does not necessarily imply that the species are valence trapped.
(12) N. S. Hush, *Prog. Inorg. Chem.*, **8**, 391 (1971).
(13) M. J. Powers, R. W. Callahan, D. N. Salmon, and T. J. Meyer, *Inorg. Chem.*, **15**, 894 (1976).
(14) J. K. Beattie, N. S. Hush, and P. R. Taylor, *Inorg. Chem.*, **15**, 992 (1975). References to related work appear here, except for the following.[15]
(15) T. C. Strekas and T. G. Spiro, *Inorg. Chem.*, **15**, 1974 (1976).
(16) G. M. Tom and H. Taube, *J. Am. Chem. Soc.*, **96**, 7827 (1974).
(17) H. Taube, *Proc. N.Y. Acad. Sci.*, submitted for publication.

Contribution from the Department of Chemistry,
Seton Hall University, South Orange, New Jersey 07079

Splitting of Hematin Dimers in Nonaqueous Solution

DAVID OSTFELD* and JANE A. COLFAX

Received July 8, 1977

The splitting of the dimer μ-oxo-bis[tetraphenylporphineiron(III)] by imidazole (HIm) and imidazolium chloride ($H_2Im^+Cl^-$) to form the bis(imidazole)iron(III) tetraphenylporphine cation was studied. In dichloromethane/nitromethane the reaction was observed to obey the rate law: $k_{obsd} = (k_1[HIm] + k_2[HIm][H_2Im^+])/(1 + K_1[HIm])$. This corresponds to a rapid equilibrium, with $K_1 = 220\ M^{-1}$, in which the μ-oxo dimer (hematin) reacts to form an adduct with imidazole. The actual splitting of the dimer then occurs by one of two kinetically indistinguishable routes. In one of these the hematin itself is split, with a rate constant equal to $(k_1[HIm] + k_2[HIm][H_2Im^+])$. In this route the imidazole adduct is unreactive. However, in the second path it is the imidazole adduct which is cleaved, with a rate constant of $(k_1 + k_2[H_2Im^+])$. The imidazole adduct is shown to resemble the adducts previously observed between the bis(imidazole) complex and either 1,10-phenanthroline or imidazole. The nature of the adduct is discussed.

Introduction

Oxo-bridged dimers of iron(III) complexes have long been known.[1] However, it was only recently that porFe^{III}–O–Fe^{III}por (por = porphyrin) (hematin) was found to be an oxo-bridged dimer and not a simple iron(III) porphyrin hydroxide.[2,3] The great stability of this dimer is a dominant feature in the chemistry of the iron porphyrins. In order to better understand why the dimer is so stable, it is first necessary to know the mechanism by which it dissociates.

Most μ-oxo dimers have been prepared and studied in aqueous solution. Their hydrolysis reactions can be described by a two-term rate law[4]

$$\text{rate} = (k_1 + k_2[H^+])[\text{dimer}] \quad (1)$$

The acid-catalyzed path, which has by far the larger rate constant, is presumed to involve the protonation of the oxo bridge followed by a rapid addition of water and cleavage of the dimer. The non-acid-catalyzed path is thought to involve the addition of a water molecule to form the unstable di-μ-hydroxo species, which rapidly comes apart.

Just such a two-term rate law has been observed for the hydrolysis of a hematin dimer in aqueous solution.[5,6] Intermediates involving iron atoms bridged by two hydroxide ions (or a hydroxide and a water molecule) have been proposed.[5] However, other studies found no evidence for them.[6]

Particularly interesting is the work of Hambright,[7] in which cyanide is present. The cleavage of hematin by HCN begins with a rapid equilibrium in which a hematin molecule reacts with a single cyanide anion. The hematin/cyanide adduct, which was spectrally observed, is then cleaved according to the rate law

$$\text{rate} = (k_1[H^+] + k_2[H^+][CN^-]^2)[\text{hematin}] \quad (2)$$

One path is simple acid hydrolysis, which is observed in any acidic aqueous solution. However, the other path involves the cyanide in a manner which cannot easily be explained. Cyanide was an interesting choice as the anion, since cyanide is a stronger complexing agent than most anions used in studies of this sort.

Much of the work done on metalloporphyrins has been done in nonhydroxylic solvents (e.g., benzene, chloroform) and this has prompted us to study hematin cleavage in such a medium. This could have been done using any of several different acids as the proton source, and we hope eventually to carry out such additional measurements. However, imidazolium chloride ($H_2Im^+Cl^-$) was chosen as a source of protons because the complexes of iron(III) porphyrins with imidazole (HIm) have been thoroughly studied and because the imidazole system is relatively easy to work with.

Experimental Section

Tetraphenylporphine (H_2TPP) was purchased from the Aldrich Chemical Co. and was converted to hematin using the method of Adler.[8] Imidazole (Eastman) was recrystallized three times from ethanol and then sublimed. Imidazolium chloride was prepared by bubbling hydrogen chloride through a suspension of imidazole in dry ether. Most of the ether was decanted off under dry nitrogen and the remainder was removed under vacuum. Imidazolium chloride is rather deliquescent, and operations involving it were carried out under inert atmosphere. All solvents were reagent grade and were used without further purification except that they were stored in stoppered flask over Linde 3A molecular sieves. Spectral measurements were made using a Beckman Acta-III spectrophotometer equipped with a temperature-controlled cell holder. Sample temperatures were maintained at 25.0 ± 0.2 °C.

Spectral measurements were made using a stock solution of hematin and a series of imidazole/imidazolium chloride solutions. In cases where 1,10-phenanthroline was added, weighed quantities were added to aliquots of imidazole/imidazolium chloride solution. After mixing, the hematin concentration was 5.55×10^{-5} M. All solutions were made using, as solvent, a mixture of equal parts by volume of nitromethane and dichloromethane. In each measurement 1.00 mL of the hematin solution was allowed to come to temperature equilibrium in a 1-cm Pyrex cuvette and then 1.00 mL of imidazole/imidazolium chloride solution was added rapidly. Mixing was complete within the few seconds it took to begin recording the spectrum.

Results

Hematin is converted, in solution with imidazole and imidazolium chloride, to the well-known bis(imidazole)iron(III) tetraphenylporphine cation—with chloride the presumed counterion. That this reaction goes cleanly and without

0020-1669/78/1317-1796$01.00/0